

Efficient current-induced domain-wall displacement in SrRuO₃

Michael Feigenson¹, James W. Reiner², and Lior Klein¹

¹*Department of Physics, Bar-Ilan University, Ramat-Gan 52900, Israel*

²*Department of Applied Physics, Yale University, New Haven, Connecticut 06520-8284*

(Dated: November 6, 2017)

We demonstrate current-induced displacement of ferromagnetic domain walls in sub-micrometer fabricated patterns of SrRuO₃ films. The displacement, monitored by measuring the extraordinary Hall effect, is induced at zero applied magnetic field and its direction is reversed when the current is reversed. We find that current density in the range of $10^9 - 10^{10}$ A/m² is sufficient for domain-wall displacement when the depinning field varies between 50 to 500 Oe. These results indicate relatively high efficiency of the current in displacing domain walls which we believe is related to the narrow width (~ 3 nm) of domain walls in this compound.

PACS numbers: 75.60.Ch, 75.75.+a, 72.25.Ba

Occasionally, the functionality of spintronic devices requires the ability to control the magnetic configuration of sub-micrometer magnetic structures. Currently, this goal is achieved in many cases (for instance in novel MRAM devices) by current lines external to the magnetic region that generate Lorentz forces; however, this method suffers from non-locality (due to the weak spatial decay of the magnetic field) and lack of scalability (since the needed current in these lines does not decrease with the magnetic bit size). Consequently, there is an intensive effort to find methods of manipulating the magnetic configuration of such structures by injecting spin-polarized electric current into the target region, a process both local and scalable. In addition to their enormous technological importance, such methods involve fascinating theoretical issues; hence, intensive theoretical and experimental efforts are invested in their study.

Two main relevant effects are considered in this respect: (a) the interaction between spin-polarized current injected into a small magnetic region and the magnetic moments of that region, and (b) the interaction between spin polarized current and a ferromagnetic domain wall. The first effect, suggested by Slonczewski [1], yields magnetic switching while the second effect, suggested by Berger [2], yields domain wall displacement. Here we address the latter effect.

Following the theoretical prediction of Berger [2], the interaction of spin-polarized current with a ferromagnetic wall has been studied both theoretically and experimentally. There have been various demonstrations of current-driven domain wall displacement [4, 5, 6, 7, 8, 9, 10, 11] using various methods for detecting the displacement, including magnetic force microscopy [4, 7], change in resistance of spin valve structures [5, 8], change in longitudinal resistance [6, 11], magneto-optics [9, 10] and Hall effect [10]. While current-driven domain wall motion in ferromagnetic semiconductor systems is achieved with moderate current density of less than 10^9 A/m² [10], the typical current density for inducing domain-wall displacement in metallic systems is in the range of $10^{11} - 10^{12}$ A/m². Domain wall displacement at lower currents densities (on the order of 10^{10} A/m²) in metal-

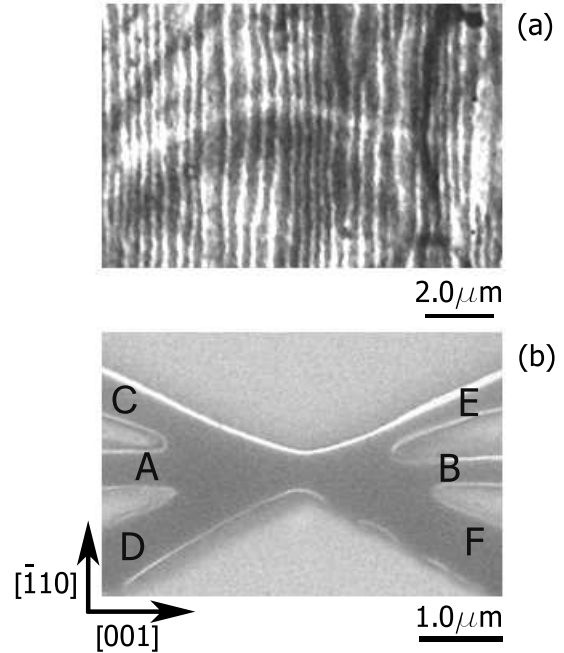


FIG. 1: (a) Image of magnetic domains in SrRuO₃ with transmission electron microscope in Lorentz mode (taken from [15]). Bright and dark lines image domain walls at which electron beam converges or diverges, respectively. Background features are related to buckling of the film and are not related to magnetic variations. (b) SEM image of the patterned sample. Current pulses are injected between A and B (perpendicular to the domain walls) and the average magnetization is sensed by measuring the extraordinary Hall effect between C-D and between E-F.

lic systems is achieved either when the depinning fields are very weak (few Oersteds) or when the domain wall resonance in its pinning potential is used [12, 13].

It has been suggested [3] that two main mechanisms are responsible for current-driven domain wall displacement: spin transfer, expected to be relevant for wide walls, and momentum transfer, expected to be relevant for narrow walls. The previously studied metallic systems are all in

the wide wall limit. Here we study current-driven domain walls in SrRuO₃ which is an excellent example of the narrow-wall limit.

We find that in SrRuO₃ depinning current (J_c) densities in the range of $5.3 \times 10^9 - 5.8 \times 10^{10}$ A/m² induce domain wall displacement where the corresponding depinning fields (H_c) are between 50 to 500 Oe. For comparison between current-induced domain-wall displacement in different systems we define H_c/J_c as a measure of efficiency and find that the efficiency in SrRuO₃ is more than an order of magnitude higher than in previously studied metallic systems of wide domain-wall ferromagnets. While we believe that the high efficiency is related to the fact that SrRuO₃ is in the narrow domain-wall limit, we find only partial agreement with relevant theoretical predictions [3].

SrRuO₃ is a metallic perovskite with orthorhombic structure ($a=5.53$, $b=5.57$, $c=7.82$ Å) and an itinerant ferromagnet with Curie temperature (for films) of ~ 150 K. Our samples are high-quality epitaxial thin films of SrRuO₃ grown by reactive electron beam coevaporation on slightly miscut ($\sim 0.2^\circ$) SrTiO₃ substrates with the [001] and $[\bar{1}10]$ axes in the film plane. These films exhibit large uniaxial magnetocrystalline anisotropy (anisotropy field of ~ 10 T) with the easy axis tilted out of the film and in-plane projection along $[\bar{1}10]$ [14]. Consequently, the Bloch domain walls are parallel to $[\bar{1}10]$ and the magnetic domains are in the form of stripes. Figure 1a shows an image from [15] of the stripe domain structure with domain width of ~ 200 nm. The image is obtained with transmission electron microscope in Lorentz mode. The width of the domain wall has been theoretically estimated to be on the order of ~ 3 nm [15] and recent experiments yield consistent results [16].

The measurements presented here are of a 375 Å - thick film of SrRuO₃ with resistivity ratio of ~ 20 - indicative of its high quality. The film was patterned using e-beam lithography followed by ion milling.

Figure 1b shows the e-beam fabricated pattern whose measurements are presented here. In our experiments we prepare a state where only a single domain wall is between terminals A and B and then we manipulate the position of the wall by injecting positive and negative current pulses (I_{AB}) between terminals A and B. The magnetic state is monitored by measuring the extraordinary Hall effect which is proportional to the average component of the magnetization perpendicular to the film plane [17]. For our purposes we always present the EHE normalized to its value when the film is fully magnetized and therefore its value reflects the ratio between domains of opposite sign in the measured area. We use the following notations: R_{EHE}^* denotes normalized EHE, and R_{CD}^* and R_{EF}^* denote the normalized EHE measured with terminals C-D and terminals E-F, respectively.

In our experimental setup we deduce the location of a domain wall by following changes in the local magnetization as determined by the EHE measurements. Therefore, it is important to have a single domain wall in the

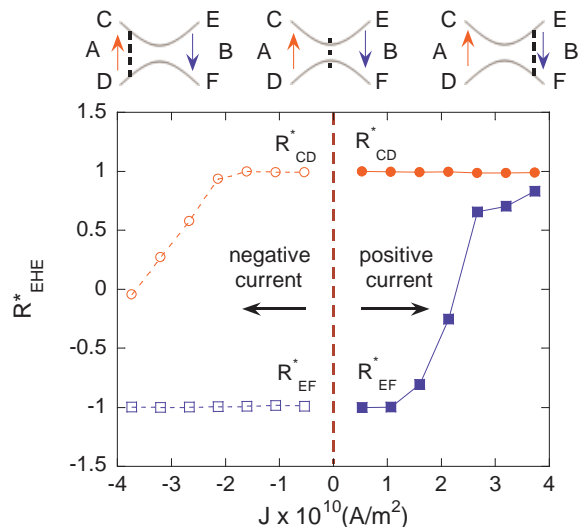


FIG. 2: Normalized EHE (R_{EHE}^*) measured with terminals C-D (R_{CD}^*) and terminals E-F (R_{EF}^*) as a function of positive and negative current pulses (100 ms) at $T=120$ K. In the initial state there is a single domain wall in the middle of the narrow constriction. The right side of the graph shows the change in R_{CD}^* and R_{EF}^* when pulses are applied from A to B. The left side of the graph starts from the same initial position and it shows the change in R_{CD}^* and R_{EF}^* when pulses are applied from B to A.

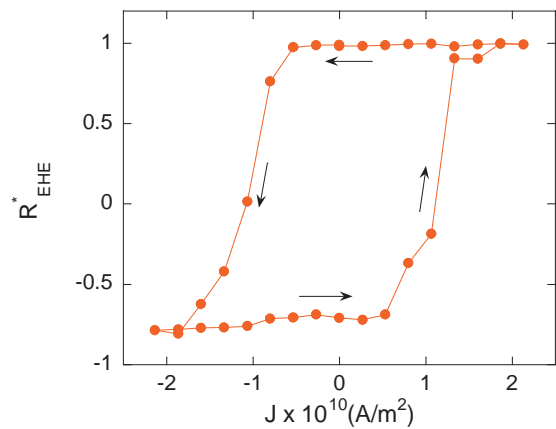


FIG. 3: Current-induced hysteresis loop with current pulses (100 ms) at $T=140$ K and $H=0$ measured with normalized EHE (R_{EHE}^*).

measured area. If there are two or more domain walls that move in the same direction in the area monitored by a certain pair of leads (C-D or E-F) their motion would not lead necessarily to change in the overall average magnetization in the measured area. Moreover, it would be impossible to deduce whether the wall moves with or against the current.

To reach a situation with a single domain wall moving between A and B we start by applying a large magnetic

field which fully magnetizes the film. Then we apply an opposite field and gradually increase its magnitude until we have nucleation of a region with reversed magnetization. The first nucleation always occurs in the left side of the pattern - between C and D and we increase the field until R_{CD}^* reaches the value of fully magnetized region, namely $R_{CD}^* = 1$, while R_{EF}^* maintains its initial value, namely, $R_{EF}^* = -1$. At this stage we decrease the magnitude of the negative field and inject current pulses of 100 ms between A and B. The magnitude of the field we leave is too small for causing wall displacement but it serves to facilitate current-induced domain wall movement that expands the magnetic domain from left to right. Figure 2 shows how this initial state is changing when current pulses are applied from A to B (the right side of the figure) and how the same initial state is changing when pulses are applied from B to A (the left side of the figure). We see that when pulses are applied from A to B, the magnetization monitored by C-D remains unchanged and above a current threshold a change in magnetization is observed in the right side of the pattern, suggesting that the domain wall at the constriction moves with the current to the right. When pulses are applied from B to A we see that the magnetization monitored by E-F remains unchanged and above a current threshold the magnetization monitored by C-D starts to decrease, suggesting that the domain wall at the constriction moves with the current to the left. The displacement occurs at higher current densities since the current is acting against the field.

With this experiment we show that with a single domain wall present we can determine that domain walls move with the current and that we can deduce domain wall displacement from average magnetization measurements.

A compelling demonstration of domain wall manipulation with current is presented in Figure 3 which shows a full current-induced hysteresis loop with $H=0$. The Figure clearly demonstrates the systematic displacement of the domain wall with current pulses applied in opposite directions.

The hysteresis loop shows that domain wall displacement is achieved only with current density above a certain threshold and that there is a typical range of currents for which significant displacement is achieved.

For quantitative study of the effect we performed similar measurements at various temperatures. Figure 4a shows typical J_c values for different temperatures. We see that J_c varies between 5.3×10^9 A/m² at 140 K to 5.8×10^{10} A/m² at 40 K.

For comparing depinning currents J_c at different temperatures and in different samples it is important to exclude the effect of the pinning potential. Since pinning potential affects depinning current as well as depinning field H_c (which is the typical field required to move domain walls) a better comparison would be by defining H_c/J_c as a measure of efficiency in displacing domain walls with current, since in this way the J_c is normalized

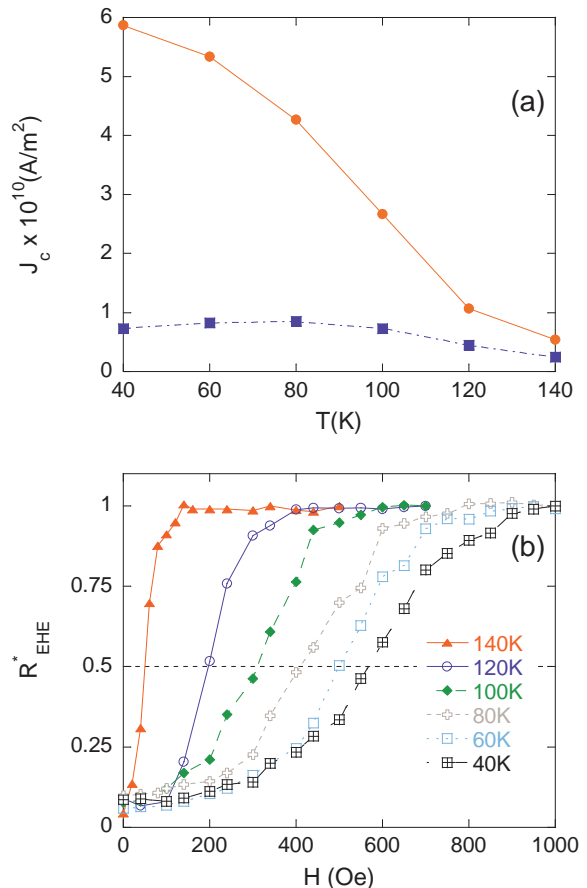


FIG. 4: (a) Characteristic measured depinning current, J_c , as a function of temperature (circles) and calculated J_c based on [3] (squares). (b) Normalized EHE as a function of applied field. The characteristic critical depinning field, H_c , for each temperature is defined as the point at which the normalized EHE is 0.5.

by the corresponding pinning potential. For this goal we measure field-induced hysteresis loops (measured with EHE). In Figure 4b we show measurements in which the sample is cooled from above T_c at zero field to a certain temperature below T_c and the magnetization is measured as a function of the applied field. We define the depinning field H_c as the field at which the magnetization reaches half of its fully magnetized state.

Using the values of the depinning fields we calculate the efficiency (H_c/J_c) in SrRuO₃ for comparison with other systems (see Figure 5). We see that the efficiency in SrRuO₃ is on the order of 10^{-12} T/[A/m²] which is more than an order of magnitude higher than the efficiency in Py (10^{-13} T/[A/m²]) as deduced from Ref. [5] and in Ni₈₀Fe₂₀ ring (10^{-14} T/[A/m²]) as deduced from Ref. [11].

A possible reason for our results is the narrow width of domain walls in SrRuO₃. Using estimated values for the exchange interaction and the magnetocrystalline anisotropy the width was calculated to be on

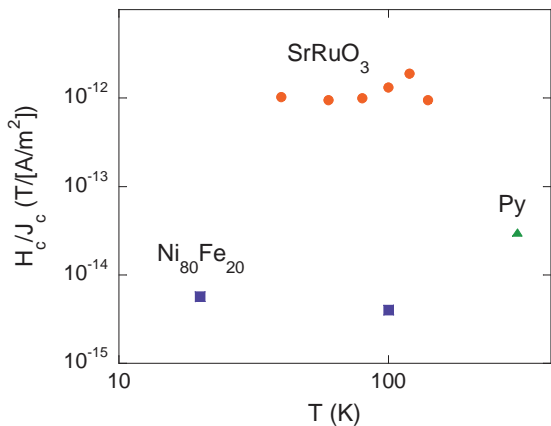


FIG. 5: H_c/J_c as function of temperature in SrRuO_3 (circles), Py (squares) and $\text{Ni}_{80}\text{Fe}_{20}$ (triangle). The data point for Py is deduced from Ref.[5] and the data points for $\text{Ni}_{80}\text{Fe}_{20}$ are deduced from Ref.[11]

the order of 3 nm, much smaller than in 3d ferromagnetic alloys. Recently, scanning tunneling spectroscopy measurements on thin $\text{SrRuO}_3 - \text{YBa}_2\text{Cu}_3\text{O}_7$ -bilayers have shown superconducting-order-parameter penetrating into SrRuO_3 in localized regions in the domain wall vicinity which puts an experimental upper bound of 10 nm on the wall width. These features make this compound a model system for studying various properties of domain walls in the ultrathin limit.

Current-induced domain wall displacement in the limit of ultrathin domain walls was considered by Tatara and Kohno [3]. The prediction is that in this limit the dominating mechanism would be moment transfer and thus $J_c = \frac{2B\mu_B}{ena^3R_wA}$ where R_w is the wall resistance, A is the cross-section area and μ_B is the Bohr magneton. In our case $na^3 \sim 1$ ($n \sim 1.6 \times 10^{28}$ [$1/\text{m}^3$][17] and $a^3 \sim 6 \times 10^{-29}$ [m^3], where n is electron density and a is the magnetic lattice constant, which is the distance between Ru ions). Two other parameters are determined experimentally: the depinning field H_c in a procedure described above (and demonstrated in Figure 4b) and the interface resistance of the domain wall in a procedure described by us before [18]. The calculated values of J_c according to this model are presented in Figure 4a for comparison with the experimental data. We find that close to T_c there is very good quantitative agreement (considering the approximations used); however, in the low temperature limit the deviation is almost an order of magnitude. Moreover, one may have expected that when moment-transfer dominates, the displacement would be with the electron current and against the nominal current. Therefore, our results indicate the need to consider other mechanisms that would be more consistent with the experimental observations.

L.K. acknowledges support by the Israel Science Foundation funded by the Israel Academy of Sciences and Humanities. J.W.R. grew the samples at Stanford University in the laboratory of M.R. Beasley.

-
- [1] J. C. Slonczewski, J. Magn. Magn. Mater. **159**, L1 (1996).
- [2] L. Berger, J. Appl. Phys. **55**, 1954 (1984); **71**, 2721 (1992).
- [3] G. Tatara and H. Kohno, Phys. Rev. Lett. **92**, 086601 (2004).
- [4] M. Tsoi, R. E. Fontana, and S. S. P. Parkin, Appl. Phys. Lett. **83**, 2617 (2003).
- [5] J. Grollier, P. Boulenc, V. Cros, A. Hamzi, A. Vaures, A. Fert, and G. Faini, Appl. Phys. Lett. **83**, 509 (2003).
- [6] M. Klaui, C. A. F. Vaz, J. A. C. Bland, W. Wernsdorfer, G. Faini, E. Cambril, L. J. Heyderman, Appl. Phys. Lett. **83**, 105 (2003).
- [7] A. Yamaguchi, T. Ono, S. Nasu, K. Miyake, K. Mibu, T. Shinjo, Phys. Rev. Lett. **92**, 077205 (2004).
- [8] C. K. Lim, T. Devolder, C. Chappert, J. Grollier, V. Cros, A. Vaures, A. Fert, and G. Faini, Appl. Phys. Lett. **84**, 2820 (2004).
- [9] N. Vernier, D. A. Allwood, D. Atkinson, M. D. Cooke and R. P. Cowburn, Europhys. Lett. **65**, 526 (2004).
- [10] M. Yamanouchi, D. Chiba, F. Matsukura, and H. Ohno, Nature **428**, 539 (2004)
- [11] M. Laufenberg, W. Buhrer, D. Bedau, P.-E. Melchy, M. Klaui, L. Vila, G. Faini, C. A. F. Vaz, J. A. C. Bland, and U. Rudiger, Phys. Rev. Lett. **97**, 046602 (2006).
- [12] E. Saltoh, H. Miyajima, T. Yamaoka, G. Tatara, Nature **432**, 203 (2004).
- [13] L. Thomas, M. Hayashi, X. Jiang, R. Moriya, C. Rettner, and S. S. P. Parkin, Nature **443**, 197 (2006).
- [14] L. Klein, J. S. Dodge, C. H. Ahn, J. W. Reiner, L. Mieville, T. H. Geballe, M. R. Beasley, and A. Kapitulnik, J. Phys. Condens. Matter **8**, 10111-26 (1996).
- [15] A. F. Marshall, L. Klein, J. S. Dodge, C. H. Ahn, J. W. Reiner, L. Mieville, L. Antagonazza, A. Kapitulnik, T. H. Geballe, and M. R. Beasley, J. Appl. Phys. **85**, 4131 (1999).
- [16] I. Asulin, O. Yuli, G. Koren, and O. Millo, Phys. Rev. B **74**, 092501 (2006).
- [17] L. Klein, J. R. Reiner, T. H. Geballe, M. R. Beasley, and A. Kapitulnik, Phys. Rev. B **61**, R7842 (2000); Z. Fang, N. Nagaosa, K. S. Takahashi, A. Asamitsu, R. Mathieu, T. Ogasawara, H. Yamada, M. Kawasaki, Y. Tokura, and K. Terakura, Science **302**, 92 (2003).
- [18] L. Klein, Y. Kats, A. F. Marshall, J. W. Reiner, T. H. Geballe, M. R. Beasley, A. Kapitulnik, Phys. Rev. Lett. **84**, 6090 (2000); M. Feigenson, L. Klein, J. W. Reiner, and M. R. Beasley, Phys. Rev. B **67**, 134436 (2003).